MOLECULAR AND CELLULAR BIOLOGY, May 2005, p. 4138–4149 Vol. 25, No. 10
0270-7306/05/$08.00+0 doi:10.1128/MCB.25.10.4138–4149.2005

ABCA5 Resides in Lysosomes, and ABCA5 Knockout Mice Develop Lysosomal Disease-Like Symptoms†

Yoshiyuki Kubo,[1]‡ Sayaka Sekiya,[1,2] Megumi Ohigashi,[1,2] Chiemi Takenaka,[4] Kyoko Tamura,[4] Shigeyuki Nada,[3] Tsuyoshi Nishi,[1,5] Akitsugu Yamamoto,[6] and Akihito Yamaguchi[1,2,4]*

Department of Cell Membrane Biology, Institute of Scientific and Industrial Research, Osaka University, Osaka 567-0047,[1] Graduate School of Pharmaceutical Sciences, Osaka University, Osaka 565-0871,[2] Department of Oncogene Research, Research Institute for Microbial Diseases, Osaka University, Osaka 565-0871,[3] CREST[4] and PRESTO,[5] JST, 4-1-8 Honcho Kawaguchi, Saitama, and Nagahama Institute of Bio-Science and Technology, Shiga 526-0829,[6] Japan

Received 22 October 2004/Returned for modification 9 December 2004/Accepted 10 February 2005

ABCA5 is a member of the ABC transporter A subfamily, and a mouse orthologue (mABCA5) in newborn mouse brain and neural cells was identified by reverse transcription-PCR. Full-length cDNA cloning revealed that mABCA5 consists of 1,642 amino acid residues and that its putative structure is that of a full-type ABC transporter having two sets of six transmembrane segments and a nucleotide binding domain. Immunohistochemical studies revealed that mABCA5 is expressed in brain, lung, heart, and thyroid gland. A subcellular localization analysis showed that mABCA5 is a resident of lysosomes and late endosomes. *Abca5*$^{-/-}$ mice exhibited symptoms similar to those of several lysosomal diseases in heart, although no prominent abnormalities were found in brain or lung. They developed a dilated cardiomyopathy-like heart after reaching adulthood and died due to depression of the cardiovascular system. In addition, *Abca5*$^{-/-}$ mice also exhibited exophthalmos and collapse of the thyroid gland. Therefore, ABCA5 is a protein related to a lysosomal disease and plays important roles, especially in cardiomyocytes and follicular cells.

*A*TP *b*inding *c*assette (ABC) transporters are membrane proteins that are widely distributed in prokaryotes and eukaryotes, and most of them transport substrates across membranes (10, 12, 35). In general, they transport drugs, toxins, peptides, lipid derivatives, and so on, coupled with ATP hydrolysis at their *n*ucleotide *b*inding *d*omains (NBDs) (12). NBDs are characterized by three motifs, Walker A, B, and C (signature) (35). In humans and rodents, ABC transporters are divided into seven subfamilies, A to G, and some of them are known to participate in physiological phenomena. In particular, subfamily A of ABC transporters is an interesting group that includes 13 members found in humans; some members of this group are known to transport lipids and their derivatives and to be related to genetic diseases (8). For example, ABCA1 has been reported to participate in cholesterol trafficking (18, 22), and a genetic defect of it causes Tangier disease, which is characterized clinically by the accumulation of cholesteryl ester in various tissues (9). ABCA1 is also involved in the engulfment of apoptotic cells by macrophages (17). ABCA4 (3, 13) is specifically expressed in the retina and transports *N*-retinylidene-phosphatidyl-ethanolamine (37), and a genetic defect of it causes Stargardt disease, which is clinically characterized by the progressive loss of central vision and progressive atrophy of the retinal pigment epithelium overlying the macula (1). These examples indicate that the physiological roles of subfamily A members are likely to differ from those of other ABC transporters, such as MDR1, for which knockout mice did not exhibit remarkable abnormalities without the administration of drugs and toxins (29). However, the functions and substrates have been determined for only two members of subfamily A.

In order to determine the physiological roles of ABC proteins in the brain or their neuron-specific functions, we tried to identify a novel member of subfamily A in newborn mouse brain and neural cells derived from P19 cells by reverse transcription (RT)-PCR. As a result of full-length cDNA cloning, we found an orthologue of human ABCA5 (mABCA5). The human and rat ABCA5 cDNA have already been isolated, and their mRNAs have been reported to be expressed mainly in brain, lung, and testis (23). The human *ABCA5* gene is located on chromosome 17q23.4 and forms a gene cluster with *ABCA6*, *ABCA8*, *ABCA9*, and *ABCA10* (10). Similar gene clustering has been found on mouse chromosome 11 (2). However, further characterization of the ABCA5 protein has not been reported. In this study, we determined the subcellular localization of the ABCA5 protein and examined its functions after generating knockout mice.

MATERIALS AND METHODS

Animals. Mice and rats were housed and handled according to the guidelines of Osaka University, complying with Japanese legislation. They were kept in a temperature-controlled environment with a cycle of 12 h of light and 12 h of dark. They received a standard diet (MF; Oriental Yeast, Japan) and water.

* Corresponding author. Mailing address: Department of Cell Membrane Biology, Institute of Scientific and Industrial Research, Osaka University, Ibaraki, Osaka 567-0047, Japan. Phone: 81-06-6879-8545. Fax: 81-06-6879-8549. E-mail: akihito@sanken.osaka-u.ac.jp.

† Supplemental material for this article may be found at http://mcb.asm.org/.

‡ Present address: Department of Molecular Biopharmaceutics, Graduate School of Natural Science & Technology, Kanazawa University, Ishikawa 920-1192, Japan.

Identification of a mouse orthologue of ABCA5 and full-length cDNA cloning. Total RNA was purified from freshly isolated brains of newborn ICR mice and neural cells derived from P19 cells induced with retinoic acid by using Sepasol (Nacalai Tesque) according to the manufacturer's instructions (15). Degenerate primers corresponding to conserved sequences of NBD1 of subfamily A, 5′-GG(T/C)CACAA(T/C)GG(A/G)GC(G/A/T/C)GG(G/C)AA-3′ and 5′-TC(G/A/T/C)GC(T/C)TC(A/G)TCCATGTG(A/G)TG-3′, were designed and used for RT-PCR to amplify the gene fragments of novel ABCA genes. The amplified fragments were ligated to the pGEM-T vector (Promega), and about 400 individual recombinant clones were sequenced with an ABI Prism 310 sequencer (Applied Biosystems). For the isolation of full-length cDNA of mABCA5, EST clones IMAGE:3025524 and RIKEN A330074A12 were obtained from Invitrogen and Y. Hayashizaki of RIKEN, respectively.

Transient and stable expression of the mABCA5 protein in cultured cells. Full-length cDNA of mABCA5 was cloned into mammalian expression vectors pcDNA3 and pcDNA5/FRT to construct pcDNA3/mABCA5 and pcDNA5/FRT/mABCA5, which were used for transient and stable expression of mABCA5, respectively. For transient expression, COS-7 cells were cultured in Dulbecco's modified Eagle medium containing 10% fetal bovine serum (FBS). For stable expression, Flp-InCHO cells (Invitrogen) were cultured in Ham's F-12 medium containing 10% FBS. Expression vectors were purified with an EndoFree Plasmid Maxi kit (QIAGEN), and transfection was performed using Lipofectamine 2000 (Invitrogen). For transient expression, cells were used at 48 h after transfection. Cell lines expressing mABCA5 stably in Flp-InCHO cells were selected and maintained in medium containing 100 to 600 μg/ml hygromycin B.

Preparation of anti-mABCA5 antibodies by the rat iliac lymph node method. The mouse myeloma cells, SP2, were provided by Y. Sado of Shigei Medical Research Institute, Okayama, Japan. The peptide of 175 amino acid residues in putative loop 1-2 region of mABCA5 was used as an antigen (Fig. 1). The region encoding the antigen was amplified by PCR and then cloned into pQE-30 (QIAGEN), a bacterial His-tagged protein expression vector. Recombinant His-tagged antigen was expressed in *Escherichia coli* strain M15 and purified on a Ni^+-affinity column. Enlarged medial iliac lymph nodes from Wistar-Kyoto rats injected via hind footpads once with an emulsion of antigen and Freund's adjuvant were used for cell fusion with the myeloma cells, SP2. SP2 cells and hybridomas were cultured in GIT medium (Wako Pure Chemicals) containing 10% FBS (28). Hybridomas producing anti-mABCA5 antibodies were screened by means of enzyme-linked immunosorbent assay and Western blot analysis.

Characterization of the anti-mABCA5 monoclonal antibody. Maltose binding protein (MBP) fusion proteins of ABCA subfamily members were constructed as follows: DNA fragments corresponding to the loop 1-2 region of mABCA5 (Pro54 to Ala228), mABCA6 (Arg52 to Ser231), mABCA8b (His51 to Ile235), and mABCA9 (Leu51 to Ser286) were amplified from mouse brain mRNAs by RT-PCR and cloned into TOPO-pCR2.1 vector (Invitrogen). The sequence of each clone was confirmed and subcloned into the HindIII and XbaI sites of pMAL-c2E vector (New England BioLabs). Each fusion protein was expressed in the *E. coli* BL21 strain carrying the pMAL plasmids encoding MBP alone, MBP-mABCA5, MBP-mABCA6, MBP-mABCA8b, or MBP-mABCA9 with IPTG (isopropyl-β-D-thiogalactopyranoside) induction, and the whole-cell lysate was prepared with sonication, followed by subjection to sodium dodecyl sulfate-polyacrylamide gel electrophoresis (SDS-PAGE) and transfer to polyvinylidene difluoride (PVDF) membranes. Western blotting was performed with anti-mABCA5 or anti-MBP antibody using rabbit horseradish peroxidase-conjugated anti-mouse IgG as a secondary antibody and the membranes were developed with ECL Plus reagent (Amersham Biosciences).

Preparation of membrane fractions. Membrane fractions were prepared from COS-7 cells transiently expressing mABCA5 and mock cells. In brief, cells were homogenized with a Teflon glass homogenizer and a tip sonicator in 15 ml of buffer A (10 mM NaCl, 1.5 mM $MgCl_2$, and 10 mM Tris-HCl [pH 7.4]) containing a protease inhibitor cocktail (catalogue number 25955-11; Nacalai Tesque) at 4°C. The homogenate was collected and centrifuged for 5 min at 1,000 rpm and 4°C. The supernatant was layered on buffer B (35% sucrose and 10 mM Tris-HCl [pH 7.4]) in a centrifuge tube and then centrifuged for 90 min at 18,000 × *g* and 4°C. The white layer at the boundary with buffer B was collected, suspended in buffer A containing a protease inhibitor cocktail, and then centrifuged for 2 h at 100,000 × *g* and 4°C. The resultant pellet was suspended in buffer A and stored at −80°C. The protein content of each preparation was determined by the Bradford method with a Protein assay kit (Bio-Rad).

Western blot analysis and *N*-glycosidase F treatment. Membrane fractions (20 μg protein) were prepared from COS-7 cells expressing the mABCA5 protein or cells carrying a mock plasmid. Membrane proteins were separated by SDS-PAGE and electroblotted onto PVDF membranes. The PVDF membranes were sequentially incubated with anti-mABCA5 rat monoclonal antibodies and the alkaline phosphatase-conjugated secondary antibodies, and then the mABCA5 proteins were visualized using CDP-Star (Amersham Biosciences). *N*-Glycosidase F treatment was performed with 4 units of *N*-glycosidase F (Roche Diagnostics) for a 3-h incubation at 37°C prior to SDS-PAGE.

Immunohistochemistry and immunostaining. Antibodies against organelle marker proteins Rab4, lysosome-associated membrane protein 2 (LAMP-2), and syntaxin 7 were purchased from Santa Cruz, and GM130 and GRP78 were from Pharmingen. Immunofluorescence staining was performed on cells grown on gelatin-coated cover glasses and frozen sections of mouse tissues. Cells were fixed in 4% (wt/vol) paraformaldehyde in phosphate-buffered saline (PBS), permeabilized with 0.1% (vol/vol) Triton X-100 in PBS, and then blocked in 0.1% (wt/vol) bovine serum albumin in PBS. Sequential incubations were performed with anti-mABCA5 monoclonal antibodies and Alexa Fluor 488-conjugated anti-rat immunoglobulin G (Molecular Probes). For double immunostaining with antibodies against organelle marker proteins, Alexa Fluor 594 or Texas Red-conjugated secondary antibodies (Molecular Probes) were used. MitoTracker staining was performed by incubating cells with 100 nM MitoTracker (Molecular Probes) in growth medium for 1 h at 37°C before fixation. The cells were mounted on slides and then examined under a confocal microscope, LSM5 Pascal (Carl Zeiss). In the case of frozen sections, samples were fixed in acetone and then blocked in 0.3% H_2O_2 in methanol. The operations after blocking were the same as those for immunofluorescence staining of cells.

Generation of ABCA5 knockout mice and quantification of thyroid hormones in plasma. For gene targeting, the embryonic stem (ES) cells, TT2 (33), were cultured in high-glucose Dulbecco's modified Eagle medium supplemented with 15% Knockout Serum Replacement (Invitrogen), leukemia inhibitory factor prepared in our laboratory, 0.1 mM 2-mercaptoethanol, 1 mM sodium pyruvate, and nonessential amino acids on the mitomycin C-treated primary fibroblasts obtained from mouse embryos at day 14 as feeder cells. ES cells (2×10^7 to 4×10^7 cells) were suspended in 500 μl of PBS containing 100 μg of linearized targeting vector and then electroporated (19, 33, 38). Homologous recombinants were screened by culturing in medium containing 200 μg/ml G418 and by PCR screening. Chimeric progenies were generated by the microinjection method, and then knockout mice were generated by mating. Development and differentiation tests for knockout mice were performed by TransGenic, Inc. Histochemical studies were performed by microscopy with hematoxylin-and-eosin- or Azan-stained sections prepared from organs after perfusion and fixation with 4% paraformaldehyde. Mouse blood sera were prepared by collecting blood from the heart and centrifugation using a MICROTAINER (catalogue number 365956; Becton Dickinson). The quantification of thyroid hormones was performed by FALCO BioSystems.

Electron microscopy. Mouse hearts were cut into small pieces in 2.5% glutaraldehyde in 0.1 M sodium phosphate buffer (pH 7.4), fixed for 2 h in the fixative, and subjected to standard electron microscopic techniques as described previously (40). Ultra-thin sections were observed under a Hitachi H7600 electron microscopy (Hitachi, Tokyo, Japan).

RESULTS

Identification of mouse ABCA5. In order to identify new members of subfamily A, which participates in brain or neuron-specific functions, RT-PCR was performed with total RNA derived from newborn mouse brain and neural cells using degenerate primers oriented to NBD1 of subfamily A. As a result, a common novel ABCA gene fragment in both RNA sources was identified.

The full-length cDNA was cloned as described in Materials and Methods. The deduced amino acid sequence of the clone revealed that it is a mouse orthologue of the human and rat ABCA5. The cloned mouse ABCA5 cDNA (mABCA5; GenBank accession number, AB097675) encodes a 1,642-amino-acid protein exhibiting 76.8% and 85.8% identity to the human and rat orthologues, respectively. Bioinformatic analysis using a program for classification and secondary structure prediction of membrane proteins indicated that the mABCA5 protein consists of 17 α-helices and two NBDs containing Walker motifs (Fig. 1A). Among these helices, 12 are proposed to be composed of membrane-spanning segments and the other 5

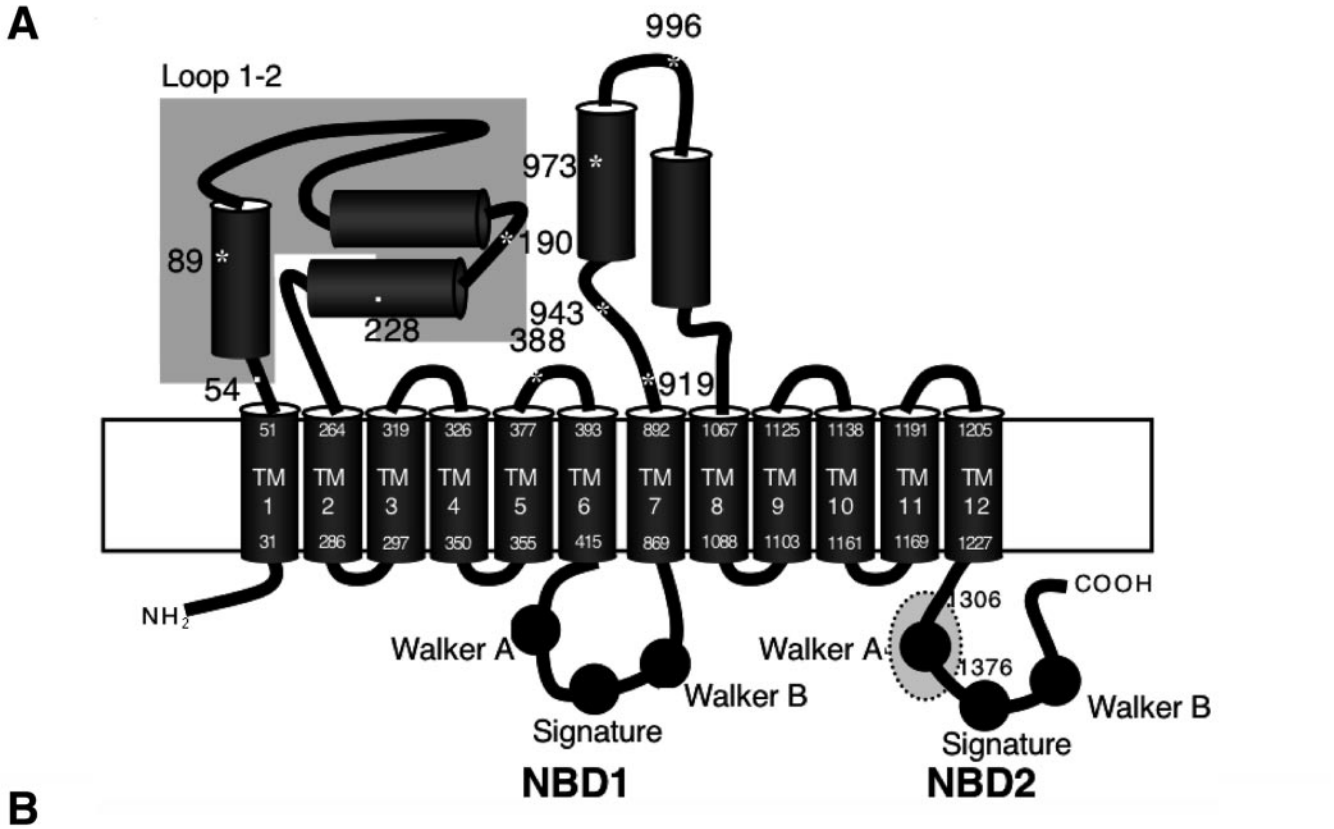

B

```
mABCA5      54 PNKKYEEVSDIELSPMDKFSLSNVILGYTPVTNITSSIMQRVSTDHLPKVIVTEEYANEKEL-VAASLSKSSNFVGVVFKDTMSYE------ 138
mABCA6      52 RNIQVLEVPPQDLGSLNEFNGSSLVVVYTPISNITQQIMNKTTFAPTMKGTRIIGVPSIEDL-DEVLLHNIPDALGVIFNDSFSYQLK---V 139
mABCA8a     52 EVYDFSSLPDVDLGRIDSFNDSTFMIVYTPITPTTQRIMDRVSLVSYMTGRKILASPNEEN-MTELISMRFSDVVGVIFTNAYSYNLKFIKG 142
mABCA8b     52 GATDLSSVPTKDLGRVDSFRQSGFMIGYTPVTSMTQQIMEKVAATPFMADKKVLGLLDEEN-IKELTESH-AEIIRVIFSDTFSYHLKFQFD 141
mABCA9      53 QVHDTPEMSVVDLGRVDNFNDSNYMMVFAPESEATHEIMNKVASAPFMKGRTIVACPDEKSMN-ELDLNYSIDAVRVIFKDTFSYHLKFSWG 143
hABCA10      1 ------------------------------------MNKMALASFMKGRTVIGTPDEETMDIELPKKYH-EMVGVIFSDTFSYRLKFNWG  28
                        ...  . . .     ...    .  .* ..     ...      . ..    ..        ..*.* ...** ...

mABCA5     139 LRFFPEMIPVSSIYMNSREGCSKT-CDAAQYWSLGFTVLQASIDAAIIQLKTNVSVWSELESTKAVIMGEAAVVEIDTFPRGVILIYLVIA   228
mABCA6     140 LRMYGNPFLKEDLLAHCWDTHSQAFCSLSKYWERGFVALQTAINAGIIEVTTNHSVMEELMSIDGINMKTLPFIPRDLSDYEIFILFCLLY   230
mABCA8a    143 ARIPTIKEHQDHTAHCHS-YGEIIYCGLSEFWRDGFVALQAAINAAIIEVTTNHSVMEEMMSLTGKYIKIDSFVGQEGTTTDCFLFFCIIR   232
mABCA8b    142 QRIPTSRELRDHNAHCDGLYED-VNCLIAIFWKEGFVALQAAINAAIIETTTNHSVMEELLSVSGKFMKIHPFVRQEGILTDFFIFTCIIS   231
mABCA9     144 QRIPKTKEHKDHSAPC-EPLNNKMICENSAFWEKGFVAFQAAINAGIIEMITNHSVMEELMSVIGSNMKMPPFIAQGGVATDFFIFFCVIS   233
hABCA10     29 YRIPVIKEHSEYTEHC-WAMHGEIFCYLAKYWLKGFVAFQAAINAAIIEVTTNHSVMEELTSVIGINMKIPPFISKGEIMNEWFHFTCLVS   143
              *..   .       .         *     *  **...*..*.*.**. .**.**..*. *   .  ..  ..          . . . .
```

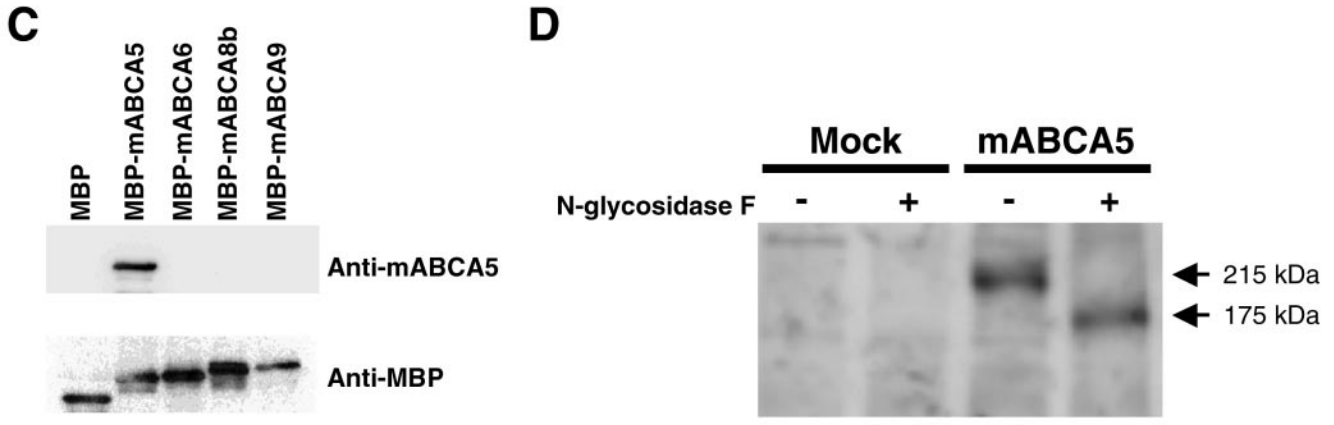

FIG. 1. Cloning and expression of mABCA5. (A) Schematic topological model of mABCA5. The cylinders and circles indicate α-helices and Walker motifs, respectively. Asterisks indicate putative glycosylation sites. The dotted gray oval on NBD2 corresponds to the region that was replaced by the neomycin resistance gene for the knockout approach. The gray box on loop 1-2 represents the region that was used for antigens for preparing monoclonal antibodies. Numbers with asterisks, cylinders, the gray box, and the dotted circle represent positions in the mABCA5

may be localized on loop domains, as judged on the sequence alignments and the predicted topologies of other full-type ABC transporters, including subfamily A. The loops between the transmembrane segment 1 (TM1) and TM2 (loop 1-2), and between TM7 and TM8 (loop 7-8) are large, containing 212 and 174 amino acid residues, respectively (Fig. 1A). There are some putative glycosylation sites in these large loops.

Expression of mABCA5 protein in COS-7 cells. The anti-mABCA5 antibody was prepared by the rat iliac lymph node method (28). In order to prepare monoclonal antibody specific to mABCA5 protein, the region between Pro54 and Ala228, which is located on the loop 1-2 (Fig. 1A), was expressed as a His-tagged protein and used for antigen preparation as described in Materials and Methods. This region has relatively low homology with other members of subfamily A (Fig. 1B). First, we tested the reactivity of the anti-mABCA5 monoclonal antibody with other members of closely related ABCA subfamily proteins by Western blot analysis using the MBP fusion proteins with the loop 1-2 region of mABCA5, mABCA6, mABCA8b, or mABCA9 (Fig. 1A and B). As we expected, no cross-reaction with mABCA6, mABCA8b, and mABCA9 proteins was observed (Fig. 1C). We then used this mABCA5-specific monoclonal antibody for Western blot analysis against the membrane fractions prepared from COS-7 cells transiently expressing the mABCA5 protein. The molecular mass of the mABCA5 protein was 215 kDa (Fig. 1D), which was significantly larger than that predicted from the amino acid sequence (185 kDa), suggesting that mABCA5 protein might be glycosylated. There are several possible glycosylation sites in the mABCA5 protein (Fig. 1A). As we expected, after *N*-glycosidase F treatment, the mobility of the mABCA5 protein on SDS-PAGE was different and the apparent molecular mass of the mABCA5 protein had decreased to 175 kDa, which is close to the predicted value, indicating that the mABCA5 protein is a glycoprotein (Fig. 1D).

Subcellular localization of the mABCA5 protein. We constructed CHO cell lines stably expressing mABCA5. Immunofluorescence analysis involving anti-mABCA5 monoclonal antibodies was performed to determine the subcellular localization of the mABCA5 protein. The staining patterns of mABCA5 comprised small punctate patterns in the cells, suggesting localization in an intracellular compartment. Costaining with GRP47, GM130, and MitoTracker, which are markers of the endoplasmic reticulum, Golgi, and mitochondria, respectively, indicated that they are not colocalized with mABCA5 protein (Fig. 2A to C). On the other hand, costaining with an antibody against LAMP-2, a marker protein of lysosomes, showed that mABCA5 protein was colocalized with it (Fig. 2D). The mABCA5 protein appeared not to be colocalized with Rab4 (Fig. 2E), a marker of early endosomes, while it was colocalized with syntaxin 7 (Fig. 2F), a marker of late endosomes. These results indicated that the mABCA5 protein is localized in lysosomes and late endosomes.

Tissue distribution of mABCA5 proteins. Transcripts of mABCA5 (10 kb) were strongly observed with brain, testis, and lung samples and weakly observed with heart, liver, kidney, skeletal muscle, and placenta samples by Northern blot analysis (see Fig. S1 in the supplemental material). Three different-sized transcripts that possibly correspond to splicing variants were observed. In testis, the low-molecular-mass transcript (6 kb) was a major transcript comparing to the others. These results were fundamentally similar to those of Petry et al. (24).

Sections of mouse tissues were stained with anti-mABCA5 monoclonal antibodies and Alexa Fluor 488-labeled secondary antibodies for detection with an immunofluorescence microscope (Fig. 3). Sections of heart, brain, and lung costained with phalloidin, proteolipid protein (PLP) (6), glial fibrillary acidic protein (32), and ABCA3 (41), which are markers of F-actin in cardiomyocytes, oligodendrocytes, astrocytes, and alveolar type II cells, respectively.

In heart, the fluorescence signal of mABCA5 protein in cardiomyocytes was observed (Fig. 3A). In brain, the fluorescence signal of mABCA5 was colocalized with PLP (Fig. 3B) and glial fibrillary acidic protein (data not shown). In lung, the fluorescence signal of mABCA5 was colocalized with ABCA3 (Fig. 3C). These results suggested that mABCA5 protein is expressed in cardiomyocytes of the heart, oligodendrocytes, and astrocytes of the brain, and alveolar type II cells of the lung. In addition, the magnified image of lung alveolar type II cells (Fig. 3D) showed that subcellular localization of mABCA5 was overlapped with the ABCA3 that is a resident of lamellar bodies known as a lysosome-related compartment of lung epithelial cells (36, 41). In liver, in contrast to these tissues, the expression of mABCA5 protein was not observed (data not shown).

Generation and characterization of *Abca5*$^{-/-}$ mice. In order to investigate the physiological roles of mABCA5, mABCA5 knockout mice were constructed from two strains, ICR and C57BL/6, as described in Materials and Methods. The targeting vector for mABCA5 gene disruption was constructed based on genome fragments of mouse ABCA5 cloned from a C57BL/6 mouse genomic library. This targeting vector consisted of 6 kb of the 3′ homologous region, 0.6 kb of the 5′ homologous region of mABCA5 gene, the neomycin resistance (Neo^r) gene cassette driven under the *pgk-1* promoter, and the subunit A of the diphtheria toxin gene cassette with PGK poly(A) driven under the MC1 promoter (Fig. 4A). With this targeting vector, the region encoding the Walker A motif of NBD2, essential for the functions of ABC proteins, should be disrupted in the mABCA5 gene (Fig. 1A). ES cells which carry

sequence. TM, transmembrane segment. (B) Amino acid sequence alignment of the antigen region between Pro54 and Ala228 of mABCA5 with the corresponding regions of mABCA6, mABCA8a, mABCA8b, mABCA9, and hABCA10. Residues that were completely conserved between species are indicated by asterisks, and four or five matches are indicated by dots. (C) Specificity of the anti-mABCA5 monoclonal antibody was checked by Western blotting. Whole-cell lysate was prepared from *E. coli* expressing MBP alone, MBP-mABCA5, MBP-mABCA6, MBP-mABCA8b, and MBP-mABCA9, as described in Materials and Methods, subjected to SDS-PAGE, and transferred to PVDF membranes. Western blot analysis was performed with anti-mABCA5 (upper panel) and anti-MBP (lower panel) antibodies. (D) Western blot analysis of mABCA5 proteins expressed in COS-7 cells with or without *N*-glycosidase F treatment. Western blot analysis and *N*-glycosidase F treatment was performed as described in Materials and Methods. + and –, with and without *N*-glycosidase F treatment, respectively.

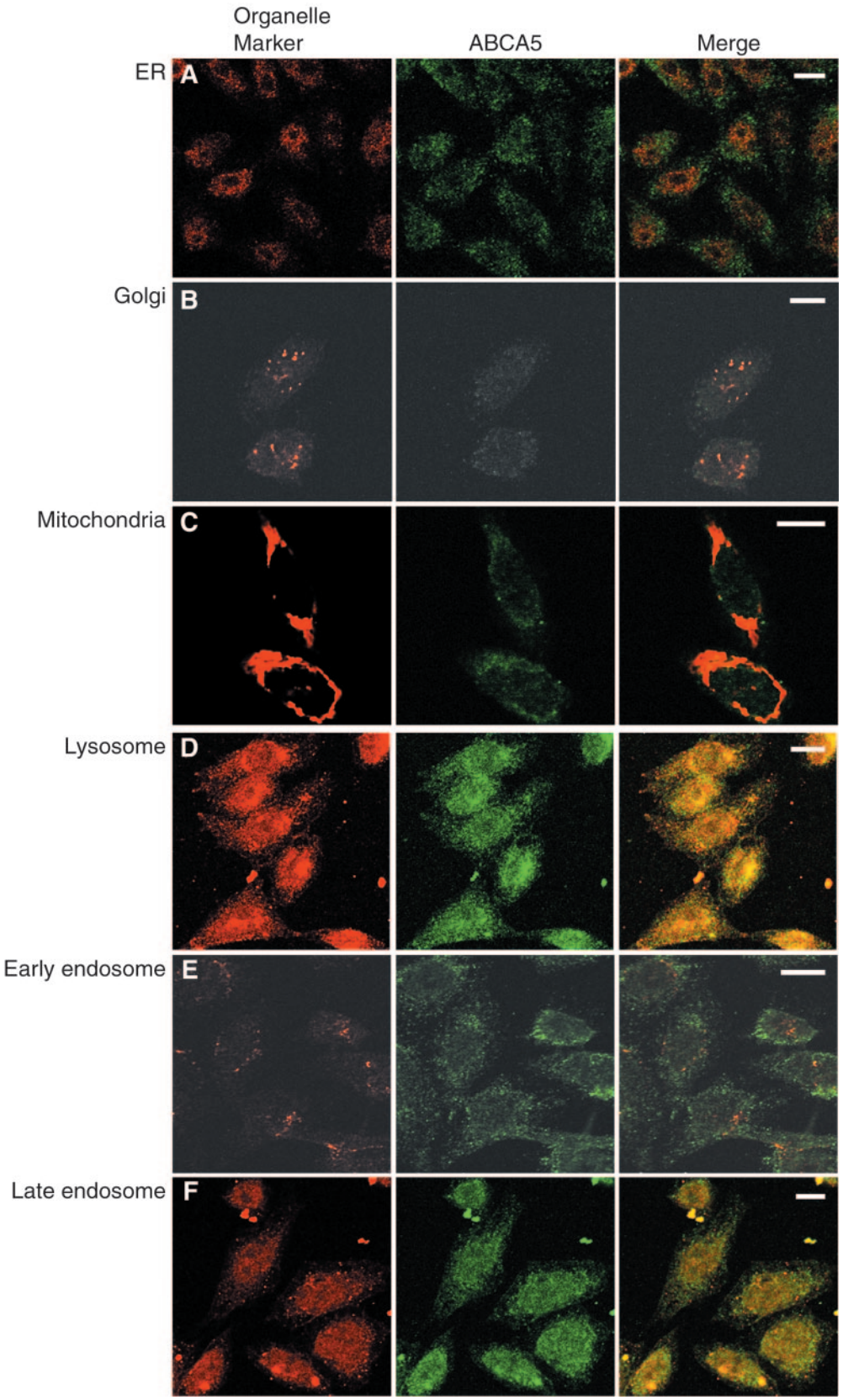

FIG. 2. Subcellular localization of mABCA5 protein. Immunofluorescence images of the CHO cells stably expressing mABCA5 proteins are shown. Cells were costained with anti-mABCA5 antibodies and a marker probe for mitochondria (MitoTracker) (C) or antibodies against marker proteins of various organelles, GRP47, GM130, LAMP-2, Rab4, and syntaxin 7, which are marker proteins of the endoplasmic reticulum (ER) (A),

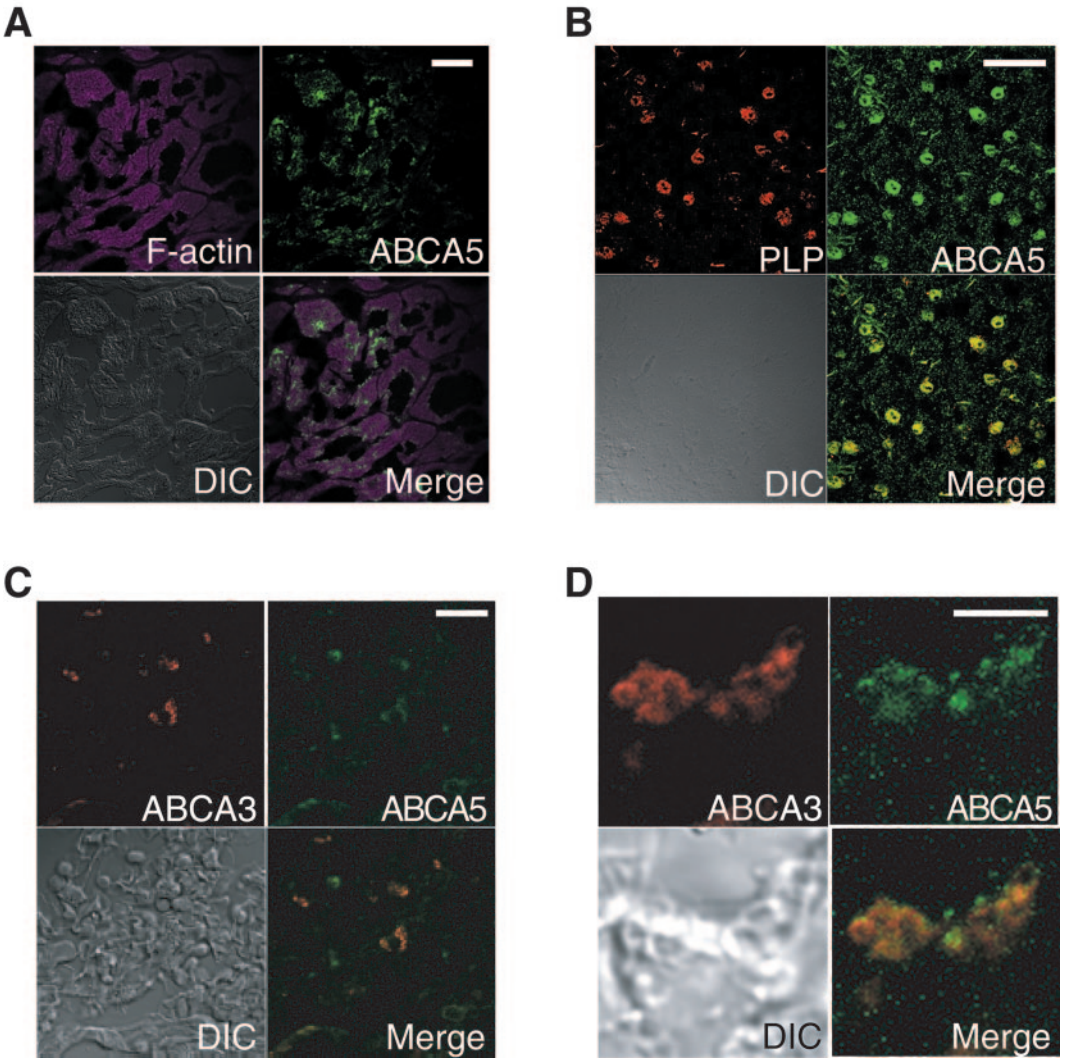

FIG. 3. Immunohistochemical analysis of mABCA5 proteins. Immunostaining images of cryosections of heart (A), brain (B), and lung (C) and the magnified image of the lung alveolar type II cells (D) are shown. All images were captured with a confocal microscope after immunostaining with anti-mABCA5 antibodies followed by Alexa Fluor488-labeled secondary antibodies. The heart, brain, and lung sections were also costained with phalloidin and antibodies against PLP and ABCA3, respectively. Green indicates mABCA5, and purple and red indicate F-actin and marker proteins, respectively. Bars, 20 μm in panels A to C and 5 μm in panel D. DIC shows differential interface contrast images.

the mABCA5-disrupted genes were screened with PCR using the forward primer 11 (5′-GAGCTGCCTGATGTGAGTGT TGGGAACCAA-3′) and the mixed reverse primers 12 (5′-T GGAATGTGCATTCCTGCCCCCAAGAAGCA-3′) for the wild-type gene and 1n (5′-GCTGCTAAAGCGCATGCTCCA GACTGCCTT-3′) for the Neo^{r} sequence inserted into the mABCA5 gene. Figure 4B shows the results of PCR screening for homologous recombinants. ES clones corresponding to lanes 3 and 7 showed the 0.85-kb product derived from the mutated locus in addition to the 1.9-kb product derived from the wild-type mABCA5 allele. After generation of chimeric progeny by means of the microinjection method, homozygous (*Abca5*$^{-/-}$) mice were obtained by mating. In *Abca5*$^{-/-}$ mice, the mABCA5 gene lacks exon 31 and parts of exons 30 and 32 corresponding to the Walker A region of NBD2 in mABCA5 protein (Fig. 1A and 4A). Their genotypes were confirmed by PCR and Southern blot analysis. The 5.4- and 2.7-kb bands correspond to the fragments derived from the wild-type and mutated loci, respectively (Fig. 4C). Heterozygous crosses showed that the distribution of the three genotypes (+/+, ±, and −/−) was according to Mendelian inheritance and that no change was observed in the gender ratio of *Abca5*$^{-/-}$ mice (male/female, 93/88), suggesting that there was no reduction in embryonal viability. In addition, the *Abca5*$^{-/-}$ mice are fertile.

After reaching adulthood, i.e., at over 10 weeks of age, the *Abca5*$^{-/-}$ ICR mice exhibited abnormalities, namely, subcuta-

Golgi apparatus (B), lysosome (D), early endosome (E), and late endosome (F), respectively. The mABCA5 proteins appear in green, each organelle marker in red, and colocalization of both fluorescents in yellow. Bars in all panels, 10 μm.

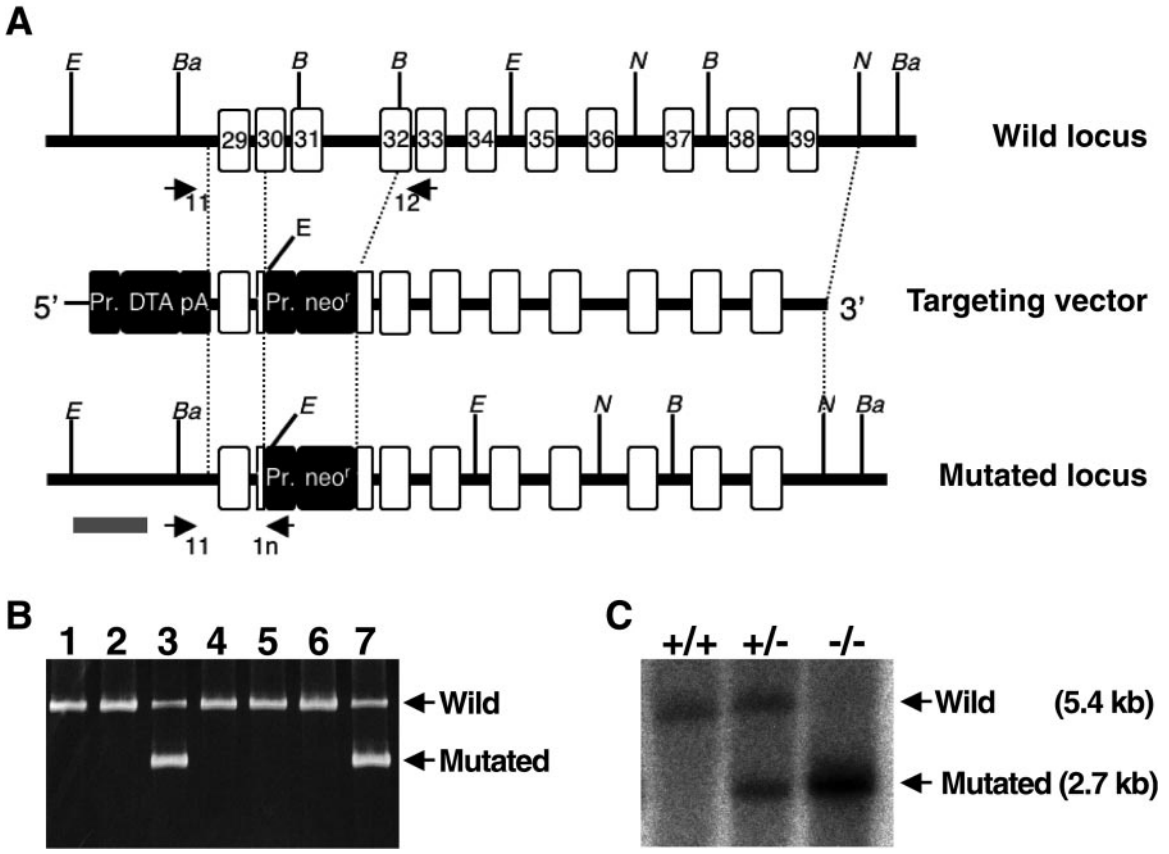

FIG. 4. Generation of *Abca5*$^{-/-}$ mice. (A) Schematic illustrations of the targeting strategy. Exons are shown as white boxes with exon numbers based on alignment of the NM_147219 and mouse genomic DNA sequences. The italic letters *B*, *Ba*, *E*, and *N* represent the restriction enzyme sites of BglII, BamHI, EcoRI, and NcoI, respectively. Closed boxes indicate the inserted gene cassettes [Pr, promoter; DTA, subunit A of the diphtheria toxin gene; pA, PGK (phosphoglycerate kinase-1) poly(A) signal; neo^r, neomycin resistance gene]. Arrows indicate the three primers, 11, 12, and 1n, that were designed for PCR screening. The gray bar represents the probe region for genomic Southern blot analysis. (B) PCR screening of ES cells. Arrows indicate the 1.9-kb and 0.85-kb PCR products derived from the wild-type mABCA5 and the mutated loci, respectively. (C) Genotyping by genomic Southern blot analysis. Genomic DNAs were digested with EcoRI, followed by detection with a [α-^{32}P] dCTP-labeled DNA probe (gray bar in panel A). Arrows indicate the 5.4- and 2.7-kb bands derived from the wild-type and mutated loci, respectively.

neous edema (Fig. 5A), exophthalmos (Fig. 5B), and trembling, and finally died. Such abnormalities were not observed for heterozygous (*Abca5*$^{+/-}$) mice. Anatomical examination of the mice that had almost died revealed an enlarged heart (Fig. 5C), an injured liver (Fig. 5D), and visceral congestion. Surprisingly, no prominent abnormalities were detected in the brain and lung sections, while mABCA5 protein was expressed in these tissues. In the liver, hematoxylin and eosin staining revealed injured tissue and an accumulation of blood cells, probably due to difficulties with the returning of the blood to the enlarged heart (Fig. 5E). Since young *Abca5*$^{-/-}$ mice sometimes showed enlarged hearts without injured livers, the heart abnormality seems to be a primary event. The liver injury might be due to congestion in the viscera caused by depression of the cardiovascular system. In the C57BL/6 *Abca5*$^{-/-}$ mice, enlarged hearts and some increases in plasma biochemical markers of liver function, glutamic pyruvic transaminase and glutamic oxaloacetic transaminase, were observed (data not shown). Severe symptoms, such as edema and liver injury, appeared only in aged mice of the ICR strain. Therefore, the appearance of symptoms seems to depend on the mouse strain.

Histochemical analysis of *Abca5*$^{-/-}$ heart. Sections prepared from wild-type and *Abca5*$^{-/-}$ mice were subjected to Azan staining. Enlarged ventricles, that is, a dilated cardiomyopathy (DCM)-like heart (Fig. 6A, right panel), and large thrombi with organization (Fig. 6B) were observed for the *Abca5*$^{-/-}$ heart, indicating that the enlarged heart is due to depression of the heart function. The organization in thrombi suggested that the depression of the heart function is a chronic symptom, not an acute one. Hematoxylin-and-eosin-stained hearts of *Abca5*$^{-/-}$ mice showed degenerated cardiomyocytes and white spots in the cardiomyocytes, suggesting that the degeneration of the cardiomyocytes is caused by vacuolation (Fig. 6C). An electron microscopic image also showed the accumulation of autolysosomes and autophagosomes in the cardiomyocytes, some of which contain myelin-like residual material. These results suggested that the vacuolation is due to abnormalities in the processing of autolysosomes (Fig. 6D).

Insights into exophthalmos in *Abca5*$^{-/-}$ mice. *Abca5*$^{-/-}$ mice also exhibited exophthalmos at the end of their lives (Fig. 5B). This symptom is often observed as Graves' ophthalmopathy in hyperthyroid patients, i.e., Graves' disease, implying a

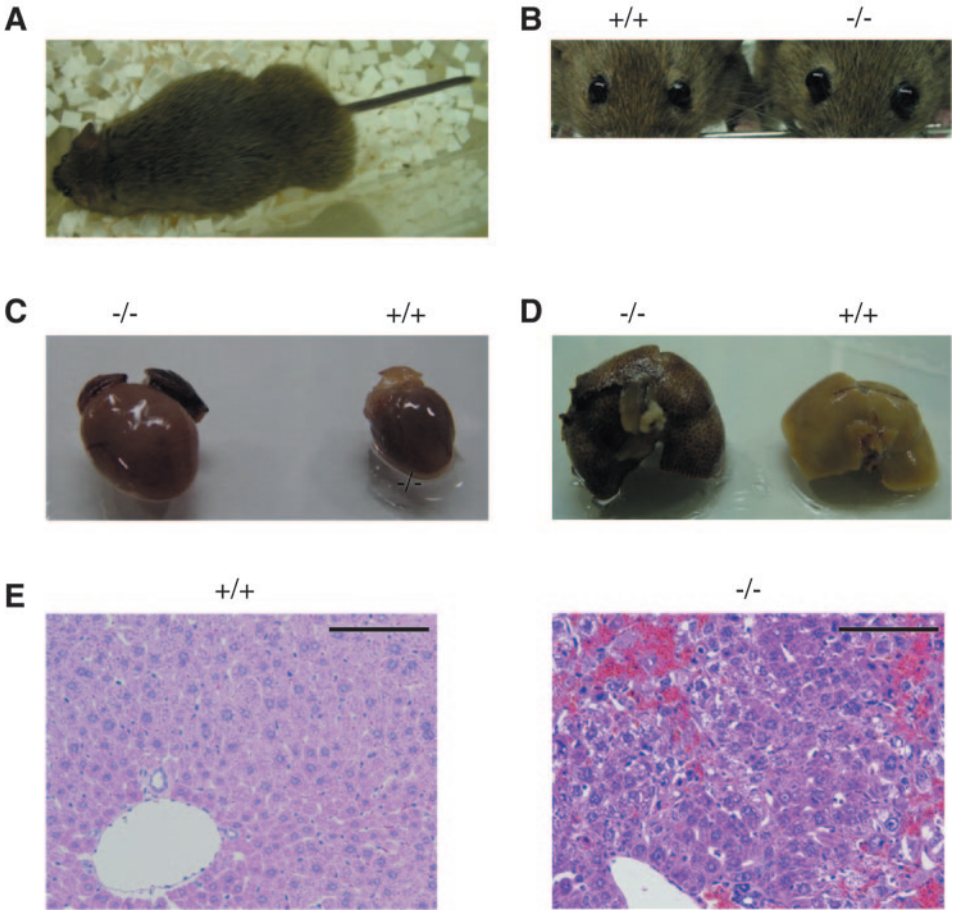

FIG. 5. Abnormalities of ABCA5-deficient mice. Weakened mice exhibited an enlarged abdomen (A) and exophthalmos (B, right) at the end of their lives. The *Abca5*$^{-/-}$ mice developed an enlarged heart (C, left) and injured liver (D, left). Anatomical observation was performed after perfusion and fixation with 4% paraformaldehyde. (E) Hematoxylin and eosin staining of the liver sections prepared from wild-type (left panel) and *Abca5*$^{-/-}$ (right panel) mice. Bars, 100 μm.

relationship between thyroid hormone secretion from the thyroid gland and mABCA5 function. On immunofluorescence staining with anti-mABCA5 antibodies and phalloidin, the fluorescence signal of mABCA5 protein was observed for follicular cells of the thyroid gland (Fig. 7A). This finding suggested a direct relationship between the ABCA5 function and thyroid hormone secretion. Thus, we determined the amounts of plasma thyroid hormones for wild-type and *Abca5*$^{-/-}$ mice. At 3 weeks of age, *Abca5*$^{-/-}$ mice showed slightly lower quantities of thyroid hormones than wild-type mice (data not shown). In the adult *Abca5*$^{-/-}$ mice that developed DCM and exophthalmos, the amounts of thyroid hormones were dramatically decreased (Fig. 7B). These results revealed that *Abca5*$^{-/-}$ mice are hypothyroid, in contrast to Graves' disease, which involves hyperthyroidism. In *Abca5*$^{-/-}$ mice, a collapse of follicles of the thyroid gland was observed with sections prepared from the knockout mice (Fig. 7C). Several *Abca5*$^{-/-}$ mice showed no detectable thyroid glands, due to complete collapse of the follicles. These results indicated that the hypothyroidism observed with *Abca5*$^{-/-}$ mice was caused by depression of the thyroid gland function.

DISCUSSION

We cloned the full-length cDNA of the mouse orthologue of human ABCA5 (mABCA5). This protein consists of 1,642 amino acid residues and is highly glycosylated (Fig. 1C). Its putative structure contains 12 transmembrane segments with two sets of NBDs and two large loop regions, like those of human and rat ABCA5.

Immunofluorescence staining with anti-mABCA5 monoclonal antibodies showed that mABCA5 protein is resident in lysosomes and late endosomes (Fig. 2). Immunohistochemical studies revealed that it was expressed in oligodendrocytes and astrocytes of the brain, epithelial cells of the lung, and cardiomyocytes of the heart. As to ABC proteins in epithelial cells of the lung, ABCA3 has been reported to exist in the lamellar body membrane of alveolar type II cells and is hypothesized to be involved in the formation of a pulmonary surfactant (14, 41). Since lamellar bodies are known to be a lysosome-related compartment (36), the colocalization of mABCA5 and ABCA3 supported the idea that mABCA5 proteins produced naturally were localized in lysosome-related organelles.

ABCA2 and ABCB9 have been reported as lysosomal ABC

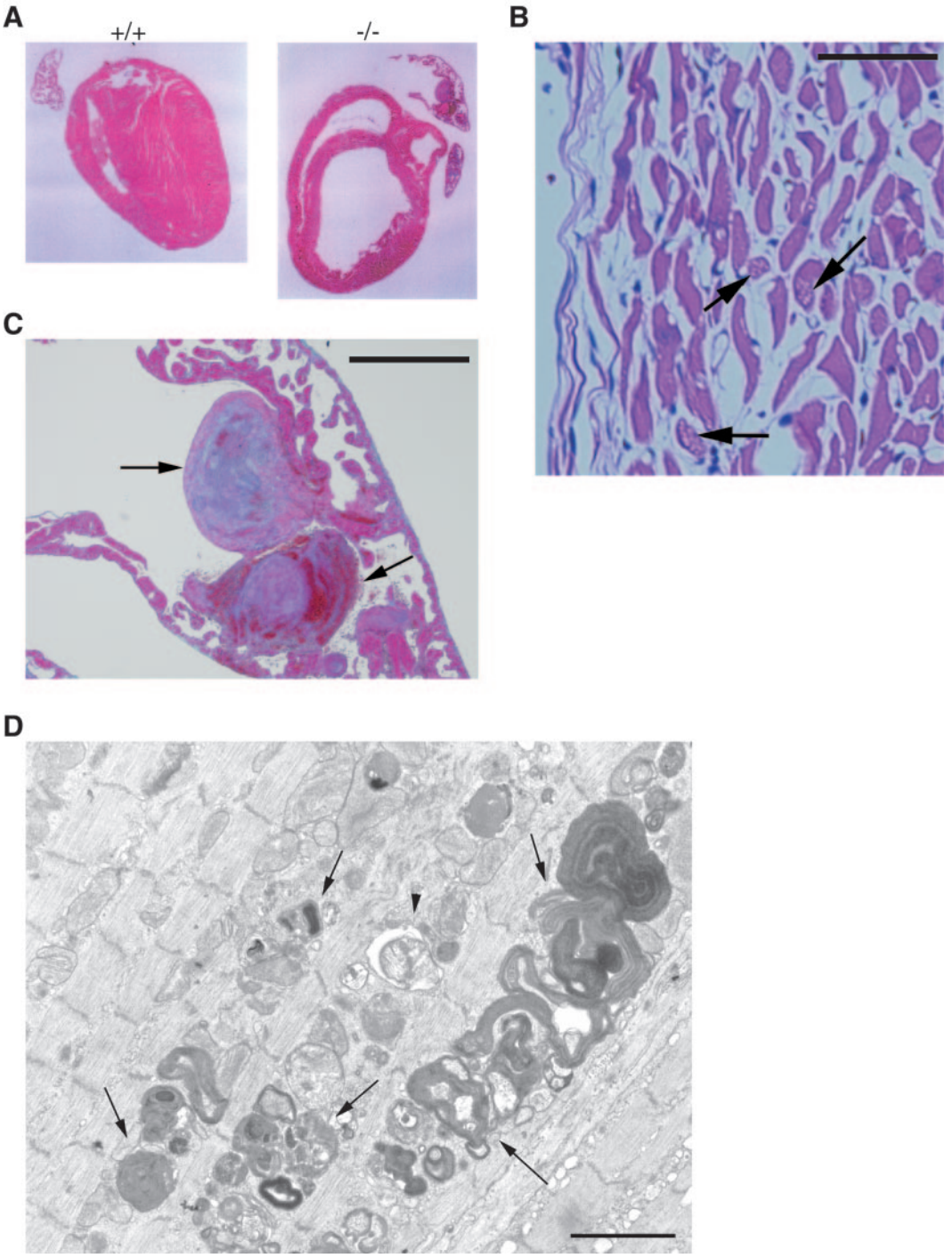

FIG. 6. Histochemical images of hearts. (A) Azan staining of the sections of heart prepared from wild-type (left panel) and ABCA5$^{-/-}$ (right panel) mice. (B) The top right part of the right panel of panel A was magnified. Arrows indicate large thrombi. Bar, 500 μm. (C) Hematoxylin and eosin staining of the cardiac muscles of *Abca5*$^{-/-}$ heart. Arrows indicate the white spots due to vacuolation. Bar, 50 μm. (D) Electron microscopic image of the section of the DCM-like heart prepared from *Abca5*$^{-/-}$ mice. Arrows indicate the accumulated autolysosomes. An arrowhead indicates autophagosome. Bar, 1 μm.

proteins (42, 43). Of these, ABCA2 has been reported to exist in oligodendrocytes (43), suggesting that ABCA5 and ABCA2 exist in the same compartment of the same cells in the brain. However, the physiological functions of ABC proteins in lysosomes remain unclear.

To elucidate the physiological function of ABCA5, *Abca5*$^{-/-}$ mice were generated. They were born and matured normally. However, after maturation, they showed prominent abnormalities, that is, they exhibited a DCM-like heart and collapse of the follicles, followed by several symptoms, includ-

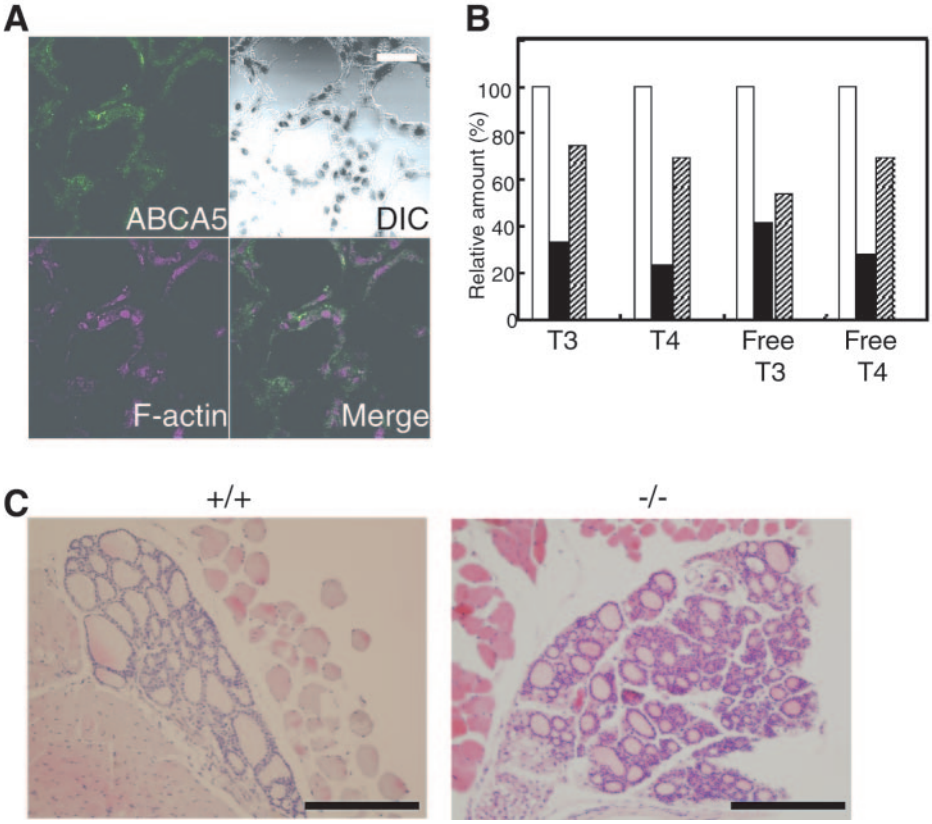

FIG. 7. Immunostaining of the thyroid glands and the level of the thyroid hormones for the wild-type and *Abca5*$^{-/-}$ mice. (A) Confocal microscopic images of the thyroid glands after immunostaining of mABCA5 using anti-mABCA5 antibodies, followed by Alexa Fluor 488-labeled secondary antibodies. F-actin was also stained with phalloidin as a control. Green and purple indicate mABCA5 and F-actin, respectively. Bar, 20 μm. (B) The relative amounts of thyroid hormones in the wild-type and knockout mice exhibiting a DCM-like heart and exophthalmos. Open bars, closed bars, and shaded bars indicate the relative amounts of thyroid hormones in plasma derived from wild-type, *Abca5*$^{-/-}$ (with DCM and exophthalmos), and *Abca5*$^{-/-}$ (with DCM only) mice, respectively. (C) Hematoxylin and eosin staining of the sections of thyroid glands prepared from the wild-type (left panel) and *Abca5*$^{-/-}$ (right panel) mice. Bars, 200 μm.

ing congestion in peripheral organs, such as the liver. The heart abnormality might appear in the early stage of life, since organization was found in thrombi in the dilated heart. Moreover, the expression of the mABCA5 protein in liver was not detected (data not shown). Heart abnormalities appear to occur prior to those of liver, since a DCM-like heart was observed for the knockout mice without injured livers. Thus, liver injury might be raised by a decreased function of the cardiovascular system. In addition, although ABCA5 is also a resident in brain and lung, no abnormalities in these organs were observed. In heart, expression levels of subfamily A mRNAs are significantly lower than that in the other organs (16). In contrast, ABCA2 and ABCA3 proteins are highly expressed in brain and lung, respectively (41, 43), indicating the possibility that other members of subfamily A may functionally compensate for the lack of ABCA5 in these organs.

With failure of the pumping action of the heart, DCM patients often show abnormalities in peripheral organs and accumulation of fluid in the abdomen (11, 25). The *Abca5*$^{-/-}$ mice exhibited edema and congestion closely resembling those exhibited by DCM patients. Viral infection, autoimmune disease, pregnancy, and exposure to toxic compounds, including alcohol, have been reported as acquired DCM initiation factors (7, 26). In addition, genetic defects, such as lysosomal diseases, also cause DCM (20, 30). Since lysosomes are the organelles responsible for the degradation of macromolecules and contain various digesting enzymes, genetic defects of lysosomal proteins often cause the accumulation of macromolecules, resulting in serious diseases. For example, GM1 gangliosidosis (OMIM 230500), Gaucher disease (OMIM 230800), and fucosidosis (OMIM 230000) are caused by the accumulation of GM1 ganglioside due to a lack of β-galactosidase, of glucocerebroside due to a lack of glucosylceramidase, and of glycoprotein due to a lack of α-fucosidase, respectively. Patients with these diseases exhibit DCM-like hearts. Interestingly, the lack of the normal function of ABCA5 also caused DCM-like hearts in *Abca5*$^{-/-}$ mice. Furthermore, Danon disease (OMIM 300257), caused by a lack of LAMP-2, is characterized clinically by myopathy and cardiomyopathy (21). LAMP-2 knockout mice show the accumulation of autophagosomes (31). Abnormalities in cardiomyocytes of LAMP-2 knockout mice also showed vacuolation caused by the accumulation of autolysosomes, similar to that in *Abca5*$^{-/-}$ mice (31). Although LAMP-2 is known to be involved in the fusion of autophagosomes and lysosomes (31), the physiological function of ABCA5 in lysosomes is unknown. ABCA5 could be

involved in the transport of materials that are essential for the processing of autolysosomes.

Abca5$^{-/-}$ mice exhibited exophthalmos similar to that of Graves' disease (4, 6). However, the plasma thyroid hormones were decreased in *Abca5*$^{-/-}$ mice, in contrast to those seen with Graves' disease, probably due to the collapse of the follicles. Abnormalities in the lysosomes of follicular cells might cause collapse of the thyroid gland, since lysosomes are responsible for the secretion of thyroid hormones (27). In Graves' disease, autoantibodies against the thyroid-stimulating hormone (TSH) receptor are produced and stimulate the TSH receptor. Stimulation of the TSH receptor causes hyperthyroidism in the thyroid gland and exophthalmos in orbital tissues (4, 6, 24). Therefore, exophthalmos is not due to surplus thyroid hormones but to stimulation of the TSH receptor in orbital tissues. Although we could not determine the amount of mouse TSH in plasma, exophthalmos in *Abca5*$^{-/-}$ mice might be caused by an increase in the amount of TSH caused by a defect in thyroid hormone secretion (34, 39). Hypothyroidism might advance gradually and be independent of depression of the cardiovascular system, since a decrease in hormones in young mice was found. The mutual acceleration of hypothyroidism and cardiovascular depression might be possible.

In summary, immunohistochemical studies and the gene knockout approach revealed the physiological importance of ABCA5 in cardiomyocytes and follicular cells, and suggested the relationship with lysosomal diseases, including DCM. The elucidation of its physiological function will lead to further understanding of functions of the ABC proteins expressed in lysosomes, the molecular mechanisms of autolysosome processing, and the mediation of lysosomal diseases, including DCM and several thyroid diseases.

ACKNOWLEDGMENTS

This work was supported by grants-in-aid from the Ministry of Education, Culture, Sports, Science and Technology of Japan, by a grant from the 21st Century COE program of the Japan Society for the Promotion of Science, and by a grant from the Core Research Evolutional Science and Technology program of the Japan Science and Technology Corporation.

We thank Aiko Yonemitsu Yuki Satsuma of Osaka University for cell biology support, Yoshikazu Sado of Shigei Medical Research Institute for instruction regarding the rat iliac lymph node method, Yoshihide Hayashizaki of RIKEN for providing the EST clones, and Chikao Yutani and Munekazu Shigekawa of the National Cardiovascular Center and Yukihiko Kitamura of Osaka University for the pathology suggestions.

REFERENCES

1. **Allikmets, R.** 1997. A photoreceptor cell-specific ATP-binding transporter gene (ABCR) is mutated in recessive Stargardt macular dystrophy. Nat. Genet. **17:**122.
2. **Annilo, T., Z. Q. Chen, S. Shulenin, and M. Dean.** 2003. Evolutionary analysis of a cluster of ATP-binding cassette (ABC) genes. Mamm. Genome. **14:**7–20.
3. **Azarian, S. M., and G. H. Travis.** 1997. The photoreceptor rim protein is an ABC transporter encoded by the gene for recessive Stargardt's disease (ABCR). FEBS Lett. **409:**247–252.
4. **Bahn, R. S.** 2002. Thyrotropin receptor expression in orbital adipose/connective tissues from patients with thyroid-associated ophthalmopathy. Thyroid **12:**193–195.
5. Reference deleted.
6. **Bahn, R. S., and A. E. Heufelder.** 1993. Pathogenesis of Graves' ophthalmopathy. N. Engl. J. Med. **329:**1468–1475.
7. **Baumann, N., and D. Pham-Dinh.** 2001. Biology of oligodendrocyte and myelin in the mammalian central nervous system. Physiol. Rev. 81. **2:**871–927.
8. **Bowles, N. E., P. J. Richardson, E. G. Olsen, and L. C. Archard.** 1986. Detection of Coxsackie-B-virus-specific RNA sequences in myocardial biopsy samples from patients with myocarditis and dilated cardiomyopathy. Lancet **1:**1120–1123.
9. **Broccardo, C., M. Luciani, and G. Chimini.** 1999. The ABCA subclass of mammalian transporters. Biochim. Biophys. Acta **1461:**395–404.
10. **Brooks-Wilson, A., M. Marcil, S. M. Clee, L. H. Zhang, K. Roomp, M. van Dam, L. Yu, C. Brewer, J. A. Collins, H. O. Molhuizen, O. Loubser, B. F. Ouelette, K. Fichter, K. J. Ashbourne-Excoffon, C. W. Sensen, S. Scherer, S. Mott, M. Denis, D. Martindale, J. Frohlich, K. Morgan, B. Koop, S. Pimstone, J. J. Kastelein, M. R. Hayden, et al.** 1999. Mutations in ABC1 in Tangier disease and familial high-density lipoprotein deficiency. Nat. Genet. **22:**336–345.
11. **Dean, M., Y. Hamon, and G. Chimini.** 2001. The human ATP-binding cassette (ABC) transporter superfamily. J. Lipid Res. **42:**1007–1017.
12. **Dec, G. W., and V. Fuster.** 1994. Idiopathic dilated cardiomyopathy. N. Engl. J. Med. **331:**1564–1575.
13. **Higgins, C. F.** 1992. ABC transporters: from microorganisms to man. Annu. Rev. Cell Biol. **8:**67–113.
14. **Illing, M., L. L. Molday, and R. S. Molday.** 1997. The 220-kDa rim protein of retinal rod outer segments is a member of the ABC transporter superfamily. J. Biol. Chem. **272:**10303–10310.
15. **Johansson, J., and T. Curstedt.** 1997. Molecular structures and interactions of pulmonary surfactant components. Eur. J. Biochem. **244:**675–693.
16. **Jones-Villeneuve, E. M., M. A. Rudnicki, J. F. Harris, and M. W. McBurney.** 1983. Retinoic acid-induced neural differentiation of embryonal carcinoma cells. Mol. Cell. Biol. **3:**2271–2279.
17. **Langmann, T., R. Mauerer, A. Zahn, C. Moehle, M. Probst, W. Stremmel, and G. Schmitz.** 2003. Real-time reverse transcription-PCR expression profiling of the complete human ATP-binding cassette transporter superfamily in various tissues. Clin. Chem. **49:**230–238.
18. **Luciani, M. F., and G. Chimini.** 1996. The ATP binding cassette transporter ABC1, is required for the engulfment of corpses generated by apoptotic cell death. EMBO J. **15:**226–235.
19. **McNeish, J., R. J. Aiello, D. Guyot, T. Turi, C. Gabel, C. Aldinger, K. L. Hoppe, M. L. Roach, L. J. Royer, J. de Wet, C. Broccardo, G. Chimini, and O. L. Francone.** 2000. High density lipoprotein deficiency and foam cell accumulation in mice with targeted disruption of ATP-binding cassette transporter-1. Proc. Natl. Acad. Sci. USA **97:**4245–4250.
20. **Nada, S., T. Yagi, H. Takeda, T. Tokunaga, H. Nakagawa, Y. Ikawa, M. Okada, and S. Aizawa.** 1993. Constitutive activation of Src family kinases in mouse embryos that lack Csk. Cell **73:**1125–1135.
21. **Nishikawa, T., and A. Takao.** 1991. Hereditary heart muscle diseases. Nippon Rinsho **49:**197–203.
22. **Nishino, I., J. Fu, K. Tanji, T. Yamada, S. Shimojo, T. Koori, M. Mora, J. E. Riggs, S. J. Oh, Y. Koga, C. M. Sue, A. Yamamoto, N. Murakami, S. Shanske, E. Byrne, E. Bonilla, I. Nonaka, S. DiMauro, and M. Hirano.** 2000. Primary LAMP-2 deficiency causes X-linked vacuolar cardiomyopathy and myopathy (Danon disease). Nature **406:**906–910.
23. **Orso, E., C. Broccardo, W. E. Kaminski, A. Bottcher, G. Liebisch, W. Drobnik, A. Gotz, O. Chambenoit, W. Diederich, T. Langmann, T. Spruss, M. F. Luciani, G. Rothe, K. J. Lackner, G. Chimini, and G. Schmitz.** 2000. Transport of lipids from Golgi to plasma membrane is defective in Tangier disease patients and Abc1-deficient mice. Nat. Genet. **24:**192–196.
24. **Petry, F., A. Kotthaus, and K. I. Hirsch-Ernst.** 2003. Cloning of human and rat ABCA5/Abca5 and detection of a human splice variant. Biochem. Biophys. Res. Commun. **300:**343–350.
25. **Rapoport, B., G. D. Chazenbalk, J. C. Jaume, and S. M. McLachlan.** 1998. The thyrotropin (TSH) receptor: interaction with TSH and autoantibodies. Endocr. Rev. **19:**673–716.
26. **Redfield, M. M., B. J. Gersh, K. R. Bailey, D. J. Ballard, and R. J. Rodeheffer.** 1993. Natural history of idiopathic dilated cardiomyopathy: effect of referral bias and secular trend. J. Am. Coll. Cardiol. **22:**1921–1926.
27. **Richardson, P., W. McKenna, M. Bristow, B. Maisch, B. Mautner, J. O'Connell, E. Olsen, G. Thiene, J. Goodwin, I. Gyarfas, I. Martin, and P. Nordet.** 1996. Report of the 1995 World Health Organization/International Society and Federation of Cardiology Task Force on the Definition and Classification of Cardiomyopathies. Circulation **93:**841–842.
28. **Rousset, B., and R. Mornex.** 1991. The thyroid hormone secretory pathway—current dogmas and alternative hypotheses. Mol. Cell. Endocrinol. **78:**C89–C93.
29. **Sado, Y., and T. Okigaki.** 1996. A novel method for production of monoclonal antibodies. Evaluation and expectation of the rat lymph node method in cell and molecular biology. Cell. Biol. Int. **20:**7–14.
30. **Schinkel, A. H., J. J. Smit, O. van Tellingen, J. H. Beijnen, E. Wagenaar, L. van Deemter, C. A. Mol, M. A. van der Valk, E. C. Robanus-Maandag, H. P. te Riele, et al.** 1994. Disruption of the mouse mdr1a P-glycoprotein gene leads to a deficiency in the blood-brain barrier and to increased sensitivity to drugs. Cell **77:**491–502.
31. **Stypmann, J., K. Glaser, W. Roth, D. J. Tobin, I. Petermann, R. Matthias,**

G. Monnig, W. Haverkamp, G. Breithardt, W. Schmahl, C. Peters, and T. Reinheckel. 2002. Dilated cardiomyopathy in mice deficient for the lysosomal cysteine peptidase cathepsin L. Proc. Natl. Acad. Sci. USA **99:**6234–6239.

32. **Tanaka, Y., G. Guhde, A. Suter, E. L. Eskelinen, D. Hartmann, R. Lullmann-Rauch, P. M. Janssen, J. Blanz, K. von Figura, and P. Saftig.** 2000. Accumulation of autophagic vacuoles and cardiomyopathy in LAMP-2-deficient mice. Nature **406:**902–906.
33. **Tascos, N. A., J. Parr, and N. K. Gonatas.** 1982. Immunocytochemical study of the glial fibrillary acidic protein in human neoplasms of the central nervous system. Hum. Pathol. **13:**454–458.
34. **Tokunaga, T., and Y. Tsunoda.** 1992. Efficacious production of viable germline chimeras between embryonic stem (ES) cells and 8-cell stage embryos. Dev. Growth Diff. **34:**561–566.
35. **Vassart, G., and J. E. Dumont.** 1992. The thyrotropin receptor and the regulation of thyrocyte function and growth. Endocr. Rev. **13:**596–611.
36. **Walker, J. E., M. Saraste, M. J. Runswick, and N. J. Gay.** 1982. Distantly related sequences in the alpha- and beta-subunits of ATP synthase, myosin, kinases and other ATP-requiring enzymes and a common nucleotide binding fold. EMBO J. **1:**945–951.
37. **Weaver, T. E., C. L. Na, M. Stahlman.** 2002. Biogenesis of lamellar bodies, lysosome-related organelles involved in storage and secretion of pulmonary surfactant. Semin. Cell Dev. Biol. **13:**263–270.
38. **Weng, J., N. L. Mata, S. M. Azarian, R. T. Tzekov, D. G. Birch, and G. H. Travis.** 1999. Insights into the function of Rim protein in photoreceptors and etiology of Stargardt's disease from the phenotype in abcr knockout mice. Cell **98:**13–23.
39. **Yagi, T., Y. Ikawa, K. Yoshida, Y. Shigetani, N. Takeda, I. Mabuchi, T. Yamamoto, and S. Aizawa.** 1990. Homologous recombination at c-*fyn* locus of mouse embryonic stem cells with use of diphtheria toxin A-fragment gene in negative selection. Proc. Natl. Acad. Sci. USA **87:**9918–9922.
40. **Yamada, M., T. Monden, T. Satoh, M. Iizuka, M. Murakami, T. Iriuchijima, and M. Mori.** 1992. Differential regulation of thyrotropin-releasing hormone receptor mRNA levels by thyroid hormone in vivo and in vitro (GH3 cells). Biochem. Biophys. Res. Commun. **184:**367–372.
41. **Yamamoto, A., R. Masaki, Y., and Tashiro.** 1996. Formation of crystalloid endoplasmic reticulum in COS cells upon overexpression of microsomal aldehyde dehydrogenase by cDNA transfection. J. Cell Sci. **109:**1727–1738.
42. **Yamano, G., H. Funahashi, O. Kawanami, L. X. Zhao, N. Ban, Y. Uchida, T. Morohoshi, J. Ogawa, S. Shioda, and N. Inagaki.** 2001. ABCA3 is a lamellar body membrane protein in human lung alveolar type II cells. FEBS Lett. **508:**221–225.
43. **Zhang, F., W. Zhang, L. Liu, C. L. Fisher, D. Hui, S. Childs, K. Dorovini-Zis, and V. Ling.** 2000. Characterization of ABCB9, an ATP binding cassette protein associated with lysosomes. J. Biol. Chem. **275:**23287–23294.
44. **Zhou, C., L. Zhao, N. Inagaki, J. Guan, S. Nakajo, T. Hirabayashi, S. Kikuyama, and S. Shioda.** 2001. ATP-binding cassette transporter ABC2/ABCA2 in the rat brain: a novel mammalian lysosome-associated membrane protein and a specific marker for oligodendrocytes but not for myelin sheaths. J. Neurosci. **21:**849–857.